



What's Constant in Contrast Constancy?

The Effects of Scaling on the Perceived Contrast of Bandpass Patterns

NUALA BRADY,*† DAVID J. FIELD*

Received 21 April 1993; in revised form 11 April 1994; in final form 21 July 1994

“Contrast constancy” refers to the ability to perceive objects as maintaining a constant contrast independent of size or distance. When tested with high contrast sinusoidal gratings, contrast constancy has been shown to hold for a wide range of spatial frequencies, suggesting that sensitivity is constant across the spectrum at suprathreshold. In this study, we show that contrast constancy also holds for relatively broadband patterns. We describe how the frequency spectra of such functions change as the patterns scale in size. In particular, we emphasize how these changes in the spectra depend on whether the functions are localized (coherent phase) or spatially distributed (incoherent phase). In Fourier terms, the scaling properties depend on the phase spectra of the patterns. Contrast constancy is shown to hold for both localized Gabor patches (coherent phase spectra) and bandpass noise patterns (incoherent phase spectra). Constancy holds over a wide range of suprathreshold contrasts; in fact, matching is quite accurate as soon as the pattern is suprathreshold. These results are explained with a model in which mechanism bandwidths increase with frequency (constant in octaves) and peak spectral sensitivity is equal across frequency out to around 16 c/deg. In the case of the Gabor stimuli, perceived contrast is assumed to be mediated by a mechanism centered on the patch. For the bandpass noise, contrast is determined by the average response of units distributed across the stimulus. This model can account for the matching data without assuming that the contrast–response gain of the underlying channels changes with spatial frequency. Neither does the model assume “response pooling”. In addition to explaining the experimental results, the model also predicts that perceived contrast will be approximately constant across scale for scenes whose spectra fall as $1/f$, as is typical of natural scenes.

Contrast Sensitivity Cortex Receptive field Natural scenes

INTRODUCTION

Much of our present understanding of contrast sensitivity in human observers comes from research motivated by linear systems theory. If a system is linear, then it is possible to derive the system's sensitivity to a set of basis stimuli and then use this profile to predict the visual response to more complex stimuli. Traditionally, sensitivity to spatial contrast has been measured using sinusoidal grating stimuli and attempts have been made to predict more general sensitivity via the application of linear systems theory (e.g. Campbell & Robson, 1968). However, the contrast sensitivity function has proved quite limited in its predictive power. One basic problem follows from the attempt to generalize from threshold to suprathreshold sensitivity. At threshold, sensitivity to sinusoidal gratings peaks around 4 c/deg and shows a significant drop at both lower and higher frequencies.

However, sensitivity at high contrasts, when measured by contrast matching, shows a much flatter function (Georgeson & Sullivan, 1975). This flattening of the sensitivity profile is also characteristic of studies in which sensitivity is measured in the presence of background noise (Daly, 1989). The term “contrast constancy” was introduced by Georgeson and Sullivan (1975) to describe the finding that high contrast gratings of different frequencies are perceived as equal in contrast when they are roughly equal in physical contrast. This finding has been reported by a number of investigators (Kulikowski, 1976; Watanabe, Mori, Nagata & Hiwatashi, 1968; Blakemore, Muncy & Ridley, 1973).

This invariance of suprathreshold sensitivity across frequency has been presumed to underlie a more interesting phenomenon: namely, that our perception of object contrast in real world scenes remains fairly stable across changes in viewing distance or scale. However, it has not always been made clear how the spectra of such objects change with viewing distance. In fact, when such details are considered, they lead to some apparent problems regarding our sensitivity to real world scenes.

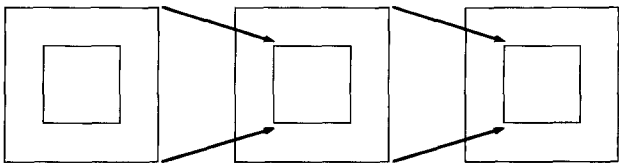
*Department of Psychology, Cornell University, Ithaca, NY 14853-7601, U.S.A.

†Present address: Vision Research Centre, Ophthalmology, McGill University, Montreal, Quebec, Canada.

The first problem results from the fact the that spectra of natural scenes are not flat. As previously noted, if the contrast energy in the environment is scale invariant (i.e. the contrast is independent of scale or viewing distance), then the spectra of natural scenes should fall in proportion to frequency (Field, 1987). Indeed, this approximate fall-off has been noted by a number of authors (e.g. Field, 1987, 1993; Burton & Moorhead, 1987; Tolhurst, Tadmor & Tang Chao, 1992). Under an application of linear systems analysis, in which a flat transfer function is assumed to characterize visual processing at high contrasts, the response of the visual system should be greatest for low frequency structure in such scenes.

Indeed, if the transfer function is flat, then we would expect the visual system’s response to natural scenes to fall as $1/f$. So for example, the response at 1 c/deg should be 20 times higher than the response at 20 c/deg in the natural environment. A second problem is that a flat sensitivity function cannot explain why our perception of contrast remains invariant when an object scales in size. As will be shown in the next section, the spectra of most scaled objects do not just shift along the frequency axes as is the case for sinusoids.

Later in this paper we will describe a model of suprathreshold contrast processing which predicts the relative perception of contrast across changes in scale for various functions. But first, it is important to understand how the spectrum of a function changes when it is scaled in size. Since the scaling relationship differs depending on whether the function is one- or two-dimensional, we describe both cases.



Scaling

FIGURE 1. Scaling in this study refers to the process of “zooming out” and re-sizing the image as shown.

SCALING IN ONE DIMENSION

When moving closer to or further from an object of fixed size, the retinal image scales in a predictable fashion. These changes can also be described in the frequency domain, in terms of the scaling of the image spectrum. The changes in the spectrum which accompany a change in image size depend upon the particular waveform that is scaled; e.g. whether it is narrow-band or broadband. As illustrated below, the scaling properties of an image also depend crucially on its phase spectrum. All of these details, which are well described with the aid of Fourier theory, are important to understanding the information available to the visual system when objects are viewed from different distances. Throughout this paper, we consider the case of “zooming out” of an image and resampling at the original resolution as shown in Fig. 1.

For sinusoidal grating patterns, such as those used in the constancy experiments discussed earlier, scaling is quite straightforward. Figure 2 shows a sequence of

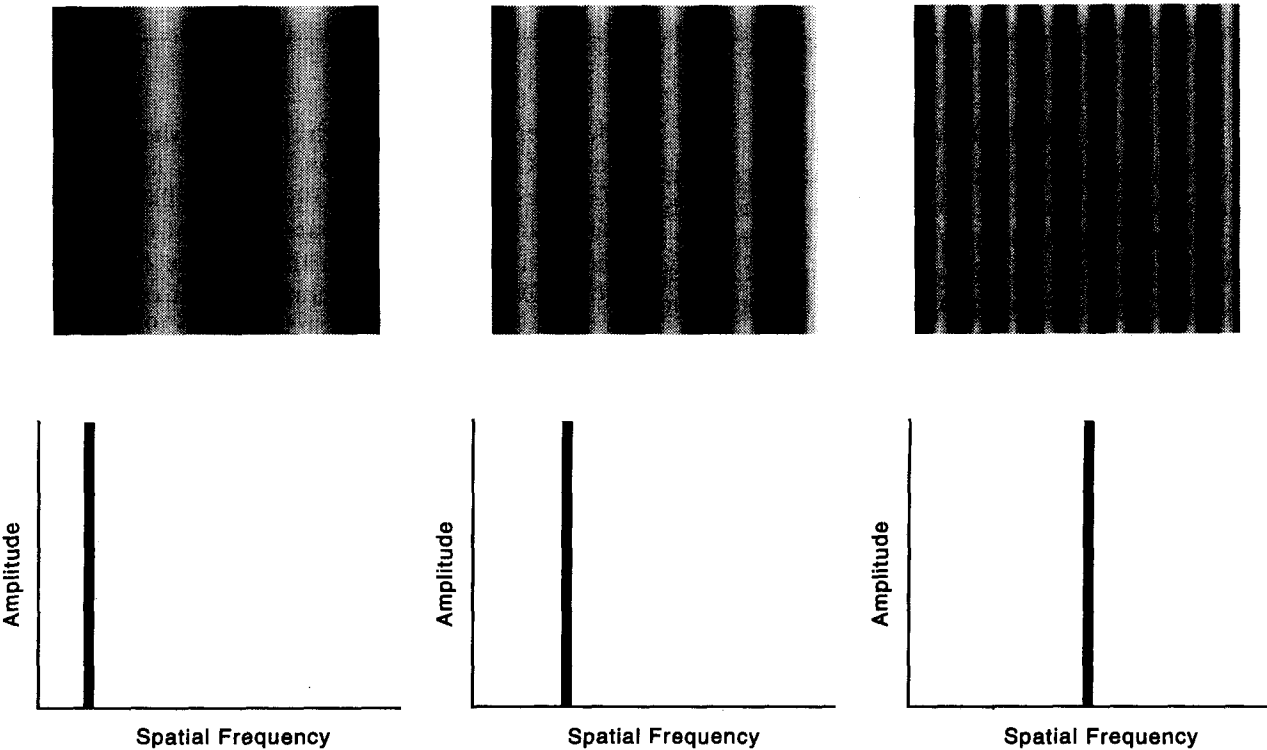


FIGURE 2. A sinusoidal grating increasing in scale. The changes in the frequency spectrum are shown on both linear (left) and logarithmic (right) axes.

gratings, which increase in frequency from left to right. For these patterns (and those in Figs 3 and 4), the change in frequency is that which results from a doubling in viewing distance with a constant angular window. The spectrum of an individual grating shows it to contain energy at a single frequency. Strictly speaking, this is only so in the ideal case of an infinitely extended grating. However, even for a localized patch of grating as shown here, the Fourier energy is located predominantly at the frequency of the grating. The scaling of such a pattern is described in the frequency domain by a shifting of the amplitude spectrum along the frequency axis. For example, as the grating gets narrower, its spectrum shifts to a higher frequency. Note that the peak amplitude of the spectrum remains constant as it shifts along the frequency axis.

The scaling properties of broadband waveforms depend on whether the functions are "localized", which in Fourier terms, is described by their phase spectra. Two types of broadband patterns are considered in this paper. In the first, the phases of all Fourier coefficients are aligned at some point. In line with optics terminology, we will refer to such a waveform as a "coherent" function. The second function considered here is one in which the phases are randomized, and this is referred to as an "incoherent" or "random phase" function. Examples of both types of pattern are shown in Fig. 3. Figure 3(A) shows a coherent function, a one-dimensional Gabor which becomes more or less spatially localized as it scales. Figure 3(B) shows an incoherent function, a one-dimensional noise pattern which remains spatially extended as it scales. When measured on a logarithmic scale (in

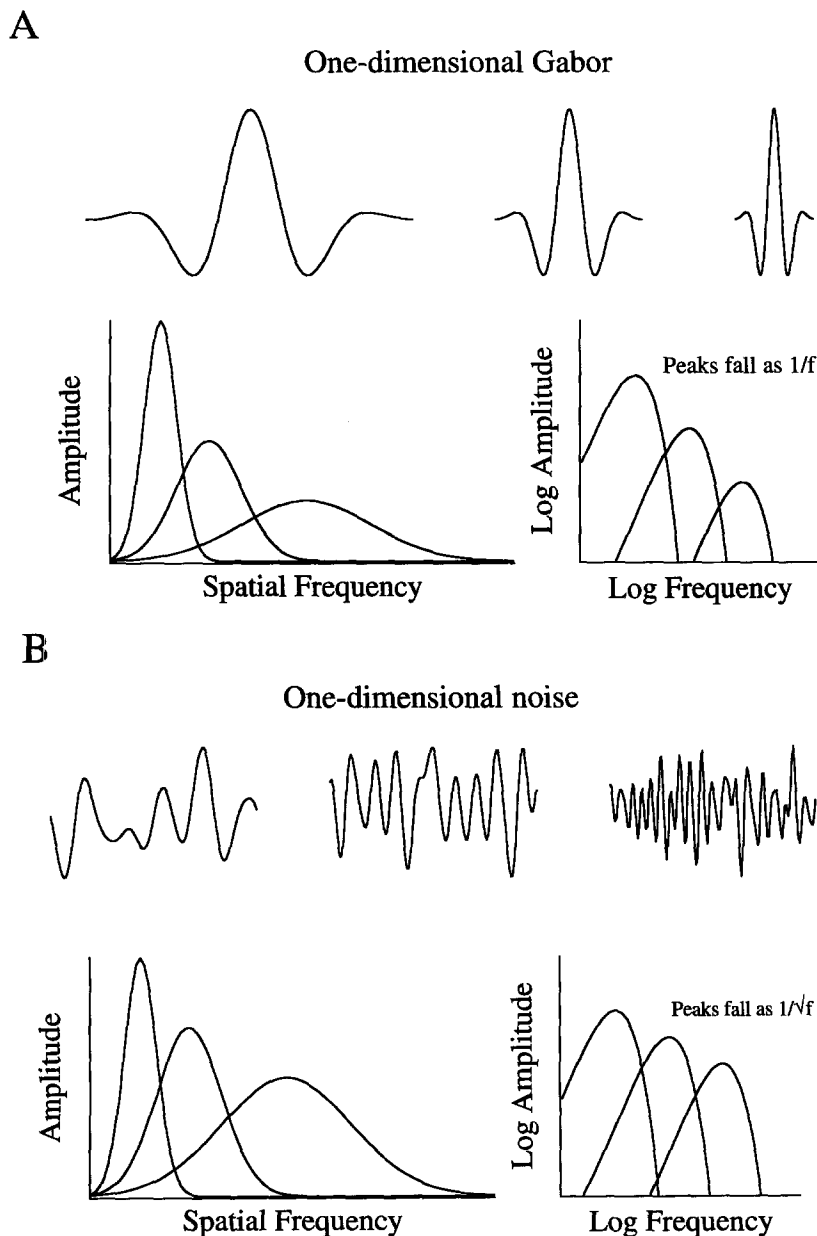


FIGURE 3. (A) A one-dimensional Gabor function scaling in width. The frequency plots show the peaks of the amplitude spectra to fall as $1/f$ on linear axes (left). This fall-off is shown by a slope of -1 on log axes (right). (B) A one-dimensional noise function scaling. The frequency plots show the peaks of the amplitude spectra to fall as $1/\sqrt{f}$ on linear axes (left). This fall-off is shown by a slope of $-\frac{1}{2}$ on logarithmic axes (right). The spectra shown are for the filters used to create these patterns.

octaves), both functions have bandwidths which are constant at different scales.

To understand the scaling of these functions, it is necessary to consider some properties of the Fourier transform. The details of what follows can be read in many texts (e.g. Bracewell, 1986). First, consider the case of the coherent Gabor function depicted in Fig. 3(A). In the space domain, this function scales by becoming either broader or narrower, while retaining a constant peak amplitude or contrast. In the frequency domain, the spectrum scales by becoming either narrower or broader while retaining a constant area. This relation is described by the similarity theorem; as a function changes in width by some scale factor, a , its spectrum changes in width by a factor $1/a$, and the peak of the spectrum changes so as to keep the area under the spectrum constant. For one-dimensional patterns, this theorem is summarized as follows;

$$g(ax) \Leftrightarrow a^{-1}G(f/a) \quad (1)$$

where $g(x)$ is the function, $G(f)$ is its spectrum and a is the scale factor. Referring again to Fig. 3(A), as the Gabor function becomes narrower, the linear bandwidth of its spectrum increases in proportion to frequency and the peak amplitude of its spectrum falls as $1/f$. Therefore, for this *coherent* function, the area under the *amplitude spectrum* remains constant across scale. The spectra are

also plotted on log-log axes on the right side of Fig. 3(A). In this plot the spectra peaks fall with a slope of -1 .

The second result from Fourier theory which is important to understanding the scaling of functions is Rayleigh's theorem. This theorem states that the integral of the squared modulus of a function is equal to the integral of its power spectrum:

$$\int |g(x)|^2 = \int |G(f)|^2. \quad (2)$$

For a discrete function this means that the area under the power spectrum is equal to the mean square value of the function. This result is often referred to as Parseval's theorem;

$$\frac{1}{N} \sum |g(x)|^2 = \sum |G(f)|^2. \quad (3)$$

Thus if two images have the same mean square value (or equivalently, the same variance or r.m.s. contrast), then the areas under their power spectra are equal.

Consider the *incoherent* noise pattern in Fig. 3(B). In the space domain, this function remains spatially extended as it scales and its variance remains constant. In the frequency domain, the area under the *power spectrum* remains constant [by equation (3)]. On a linear frequency axis, as the bandwidth of the spectrum

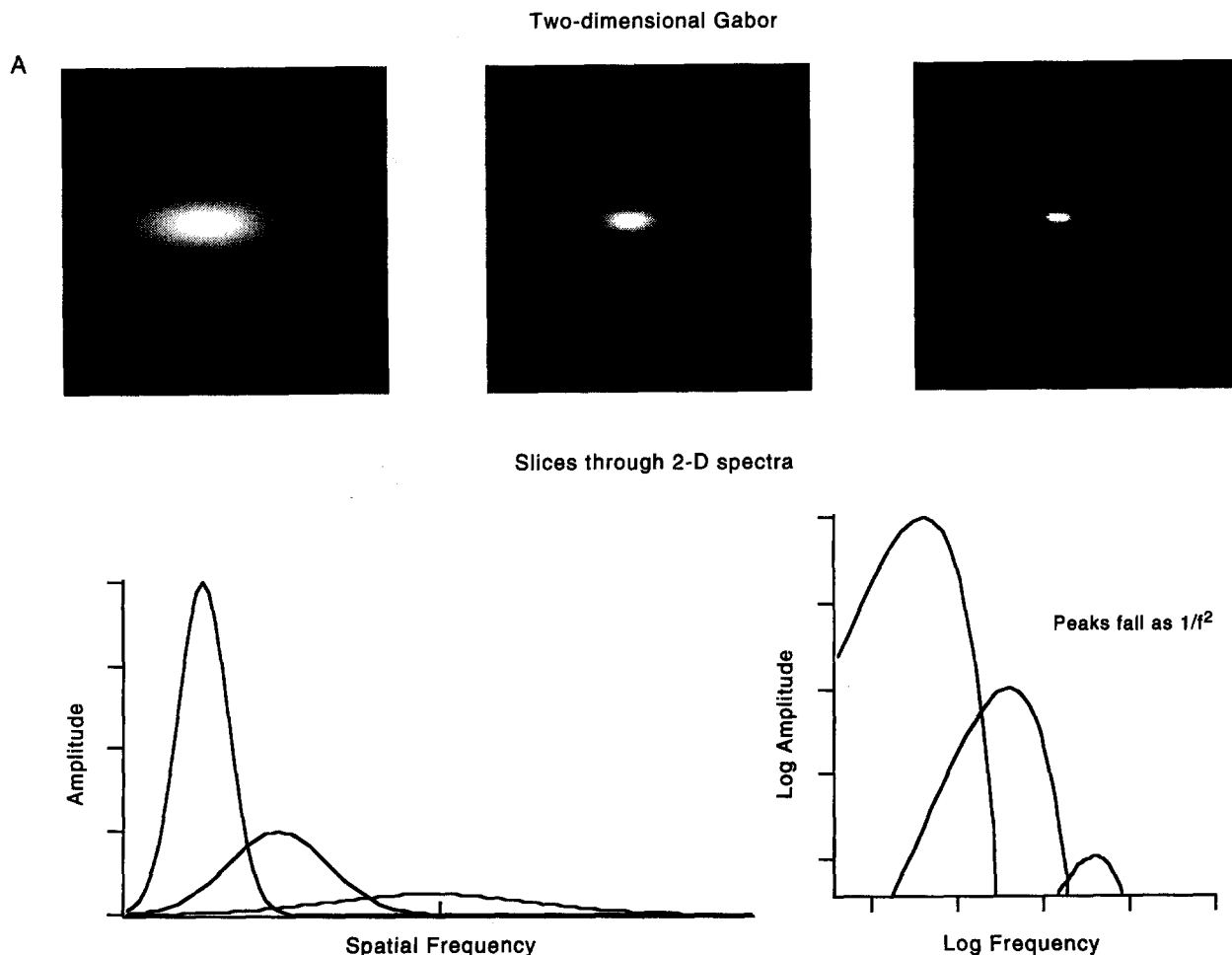


Fig. 4—Caption on facing page.

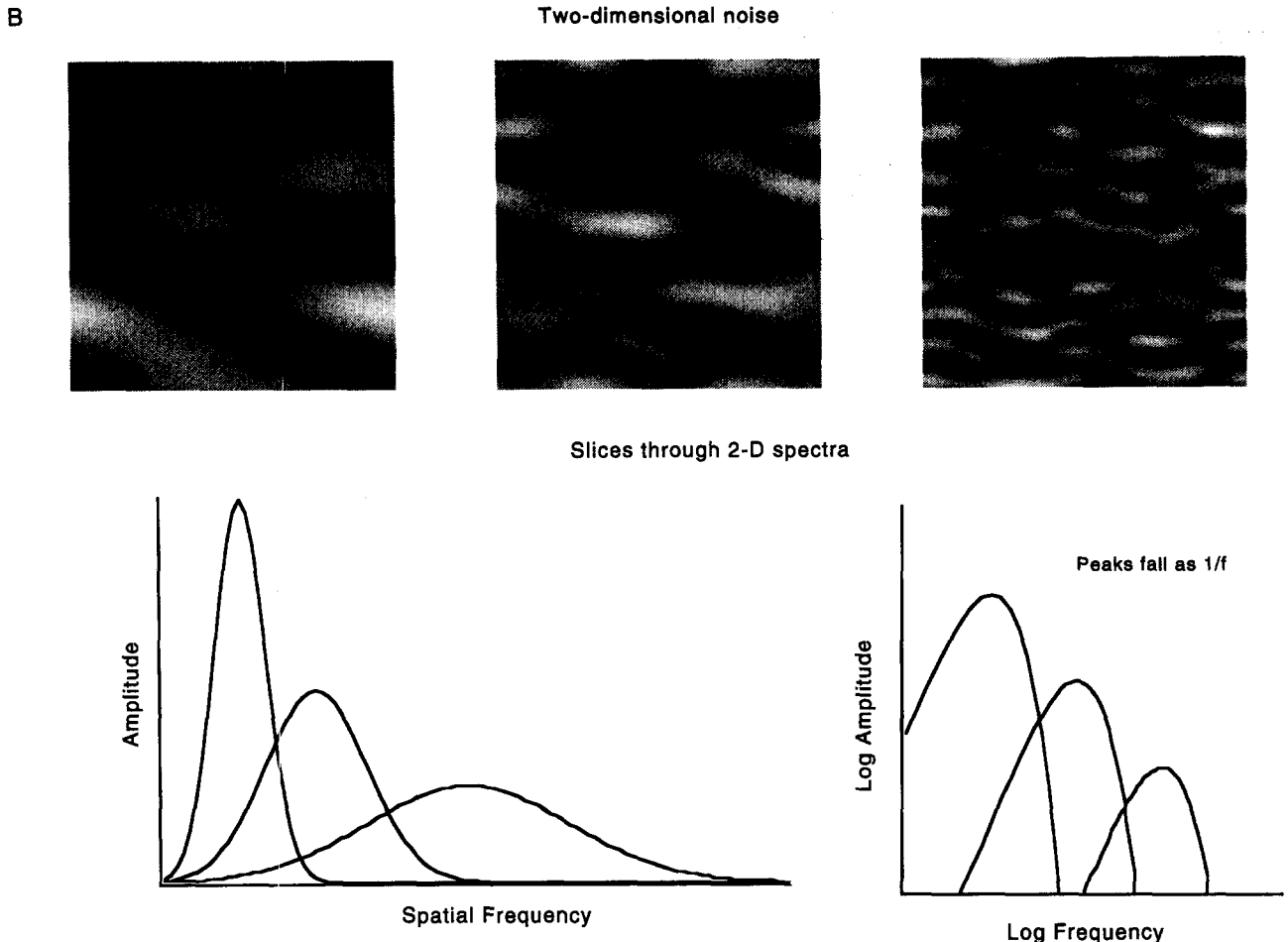


FIGURE 4. (A) Examples of two-dimensional Gabor patches used in Expt 2, with frequency increasing from left to right. The frequency plots (one-dimensional slices through the two-dimensional spectra) show the peaks of the amplitude spectra to fall as $1/f^2$ on linear axes (left). This fall-off is shown by a slope of -2 on log axes (right). (B) Examples of two-dimensional filtered noise patterns used in Expt 1 with frequency increasing from left to right. The frequency plots (one-dimensional slices through the two-dimensional spectra) show the peaks of the amplitude spectra to fall as $1/f$ on linear axes (left). This fall-off is shown by a slope of -1 on log axes (right). The spectra are for the filters used to create the patterns.

increases with frequency, the peaks of the power spectra must fall as $1/f$ to keep this area constant. Therefore, as shown on the left of Fig. 3(B), the peaks of the amplitude spectra fall as $1/\sqrt{f}$. On log-log axes, the slope of the function relating peak amplitude and frequency is $-\frac{1}{2}$.

SCALING IN TWO DIMENSIONS

The logic of scaling in two dimensions is essentially the same, except that in two dimensions the integral under the spectrum now refers to a volume rather than to an area. First consider the random phase noise pattern in Fig. 4(B). For these extended functions, the variance, and therefore the volume under the power spectrum remains constant across scale. Because the area under the spectrum increases with the square of frequency, the peaks of the power spectra must fall as $1/f^2$ to retain a constant volume. As shown on the left of the figure, this results in the peaks of the amplitude spectra falling as $1/f$. This $1/f$ fall-off is shown as a slope of -1 on the log-log plot of the spectra.

For a localized function, such as the two-dimensional Gabor pattern in Fig. 4(A), the scaling relations are described by the similarity theorem as

$$g(ax, ay) \Leftrightarrow a^{-2} G(u/a, v/a). \quad (4)$$

In the example shown, the Gabor patch becomes narrower in both spatial dimensions, x and y . Its spectrum becomes correspondingly wider in frequency, and the peak of the spectrum falls in such a way as to keep the volume under the amplitude spectrum constant. Since the area of the spectrum under the filter increases with the square of the frequency, the peak of the amplitude spectrum must fall as $1/f^2$ to keep this volume constant. As shown on the right of the figure, the slope of the function relating peak amplitude and frequency is -2 on log-log axes.

To summarize, the spectra of coherent and incoherent functions show different but consistent changes as they scale. As one "zooms out" from these patterns, their spectra shift to higher frequencies and increase in frequency bandwidth. For functions with coherent phase spectra, the peaks of the spectra fall so that

the volume under the amplitude spectrum remains constant across scale. For functions with incoherent phase spectra, the peaks fall so that the volume under the power spectrum remains constant with scale. If contrast constancy holds for these patterns, then they should appear equal in contrast at the different scales depicted in Fig. 4. The following psychophysical experiments investigated the perceived contrast of these patterns at different spatial frequencies.

EXPERIMENTS

In the three experiments reported below we used a contrast matching task to investigate relative sensitivity to contrast with bandpass patterns, across a range of spatial frequencies and at a variety of suprathreshold contrasts. In Expts 1 and 2, matching was performed at three suprathreshold contrast levels with random phase and coherent phase stimuli respectively. The purpose of Expt 3 was to investigate more thoroughly the effect of standard contrast on the scaling of visual sensitivity to contrast. In the following section we describe the methods which were common to all experiments.

Methods

Stimuli. The stimuli consisted of either bandpass noise patterns (Expt 1) or localized Gabor functions (Expts 2 and 3), examples of which are shown in Fig. 4. The noise patterns were generated by filtering a white noise image with Gaussian bandpass filters, and the Gabor functions were generated by filtering a single spot on a uniform background using the same set of filters. The filters are described in the frequency domain as

$$H(u, v) = A \times \exp [-((u - f_0)^2 + v^2) / (2 \times \sigma^2)] \quad (5)$$

where f_0 is the central frequency of the filter, A is the amplitude and σ is the SD. The spectra of the filters were Gaussian in two dimensions and the filter orientation was vertical. The frequency bandwidths of the filters, as measured by W (full width at half height, where $W = 2.35 \times \sigma$) were set equal to the peak frequencies, resulting in a 1.6 octave bands for all stimuli.

Display. All experiments were run on a Sun Sparc 10 workstation, using a color display with an 8-bit pixel depth. Each of the color guns was capable of 8 bits of gray level. The number of gray levels was increased from the usual 256 to a total of 1024 using a "bit stealing" method. Different subsets of 256 linearly spaced gray levels were used to display the stimuli. For example, in Expts 1 and 2 contrast matching was performed at three standard contrast levels. The 8 bits were selected from the full 10-bit luminance range for the high contrast condition, from the middle 60% of the range for the intermediate level, and from the middle 40% of the range for the lowest standard contrast. Choosing the 8 bits from a small inner luminance range allows for increased resolution of the low contrast stimuli, but also limits the highest contrast available for matching. This was not a problem in any of the experiments as the standard

contrasts were chosen with regard to the limits allowed by the modified display, i.e. we ensured that an adequate range of contrasts, both higher and lower than the standard, was available to the subjects as potential matches.

The screen resolution was 1150×900 pixels, and the monitor subtended 9.0 deg wide and 7.0 deg high at a viewing distance of 1.89 m. The images were 512×512 pixels (approx. 13.2×13.2 cm) and were presented side by side with a separation distance of 0.5 deg. All images were displayed at a mean luminance of 55 cd/m² and the background was set to this mean value.

Procedure. The same experimental procedure was employed in all three experiments. Observers were presented with pairs of stimuli and were asked to adjust the contrast of the "variable" stimulus until it was perceived as equal in contrast to the "standard" stimulus. Subjects were given unlimited time to make a match. Viewing conditions were normal and there was no fixation point. Contrast adjustments were made using the workstation mouse, and subjects were required to bracket their chosen contrast match, i.e. to adjust the variable stimulus contrast to higher and lower values before deciding on a final match. In a pilot experiment, matches were sometimes reported to be difficult at high spatial frequencies. Therefore, in these experiments, subjects' comments were noted in cases of difficult matches.

Observers. Five observers were run in Expts 1 and 2 and two observers were run in Expt 3. All had either normal or corrected-to-normal visual acuity. One of the authors, NB, participated in all three experiments. All other observers were naive as to the aim of the experiments.

Experiment 1—Bandpass Noise Patterns

In Expt 1, the stimuli consisted of 1.6 octave noise patterns centered at frequencies of 0.5–32.0 c/deg in octave steps. Three frequencies (0.5, 1.0 and 2.0 c/deg) were tested at a near viewing distance of 1.9 m and six frequencies (1.0–32.0 c/deg) were tested at a far distance of 3.8 m. The noise patterns subtended 4 deg of visual angle both horizontally and vertically at the near distance. Because of the size of the screen we were restricted to using noise patterns of the same absolute dimensions in the near and far conditions. This means that the visual angle subtended by the patterns in the far condition was half that of the corresponding angle in the near conditions. As discussed below, the data appear to show no evidence of an effect of unequal spatial extent across the two viewing conditions.

Subjects were required to match the contrast of each test patch to a 4 c/deg standard which was set to one of three suprathreshold contrasts, corresponding to r.m.s. contrasts of 0.03, 0.08 and 0.19. In all three contrast conditions, the initial test contrast was randomly set to between $\pm 25\%$ of the standard. The contrast of the test stimulus was then increased or decreased by 5% of its current value in response to

observer input. Within each of the three contrast conditions, the order in which the frequencies were tested was randomized.

Results

The results for Expt 1 are shown in Fig. 5. The data are plotted in two different ways. On the top, in Fig. 5(A), the data are plotted so as to emphasize the spectral changes which characterize the scaling of the stimuli. For each of the three contrast conditions, the peak of the amplitude spectra (when the patterns were matched for apparent contrast) is plotted against the spatial frequency of the peak. On the right, in Fig. 5(B), the data are plotted in terms of the more conventional "isoresponse" plots. Here, the r.m.s. contrast required for a perceptual match with the standard is plotted as a function of spatial frequency.

Each data point is the mean for all subjects and the error bars indicate ± 1 SE. Solid symbols indicate

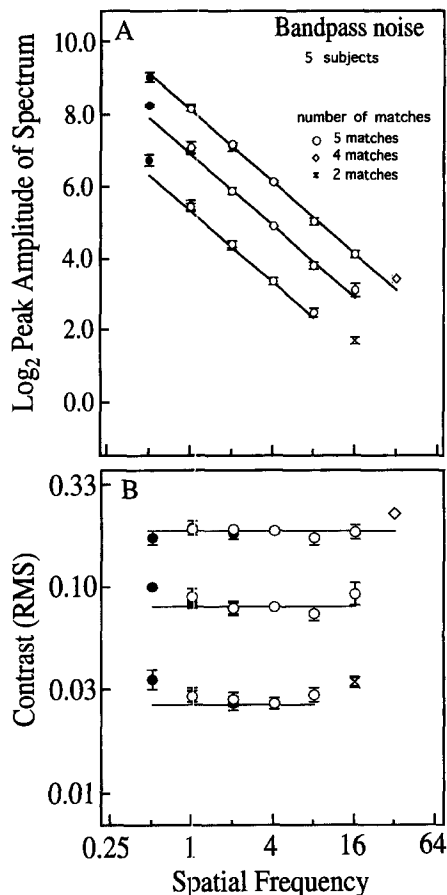


FIGURE 5. Contrast matching data for the noise patterns (Expt 1) at three suprathreshold contrasts. The same data are plotted in two ways. In (A), the peak of the amplitude spectra (when the patterns were matched for apparent contrast) is plotted against the spatial frequency of the peak. In (B) the contrast required for a perceptual match with the standard is plotted as a function of spatial frequency. Subjects adjusted the contrast of the test frequency to match the contrast of the 4 c/deg standard. The solid symbols show results of the near condition while the open symbols show results for the far condition. Results were not included if the subjects stated that they could not make an acceptable match. This resulted in a lower number of matches at the highest frequencies. The solid lines in both plots show predicted constancy.

frequencies tested at the near distance and open symbols indicate those tested at the far distance. In general, the SE was low and all subjects reported that they found the task easy to perform. A few exceptions occurred at the highest spatial frequencies, where matching was sometimes reported to be difficult or impossible. This information is included in the plots. For example, most data points in Fig. 5 are marked by a circle, indicating that all five subjects made a match. Different symbols are used to indicate frequencies at which one or more subjects could not make a match (see legend for details). Within the range of frequencies tested (0.5–32.0 c/deg) the absence of a data point indicates that no subjects could make a match at that frequency. Where matching was impossible, the variable stimulus was reported to change from being visible and of higher contrast than the standard to a state in which it could not be matched. In this state, the noise patterns were reported to be "almost invisible" or "to fade in and out of appearance" or "to no longer look the same" (e.g. regions of the patterns were sometimes reported to disappear or fade). It should be stressed here that such difficulties were atypical of the matching process in general.

The results show that observers demonstrate contrast constancy with these patterns. Referring first to Fig. 5(A), the peak of the spectra were adjusted to lower amplitude with increased spatial frequency, as is expected for constancy. The three solid lines in Fig. 5(A) have a slope of -1.0 and are included to show how the peaks fall when the patterns are exactly scaled. In this case, the patterns would have the same variance or r.m.s. contrast. The slopes of the best fitting lines to the data come close to this ideal and were approx. -1.0 for all three contrast levels. Both near and far conditions produce comparable results: the 1 and 2 c/deg data collected at the different distances overlap. In Fig. 5(B), perfect matches would fall along the series of straight dotted lines and as can be seen, the data conform pretty well. Departures from constancy are more obvious in this plot and occur at both the highest and lowest spatial frequencies at which matches were made. In all these cases, subjects set the variable stimuli to a higher physical contrast than expected for contrast constancy.

As the standard contrast changes from high to low, a pattern of responding is clearly visible in both plots. The upper frequency at which contrast matching is possible decreases gradually. This is evidenced by both a leftward shift in the frequency at which all subjects could make a match, and by a decline in the number of subjects who made a match at the highest frequency.

Experiment 2—Gabor Patches

In Expt 2 the stimuli consisted of 1.6 octave Gabor patches centered at frequencies of 0.5–32.0 c/deg in octave steps. Subjects were required to match the contrast of each test patch to a 4 c/deg standard which was set to one of three contrasts, corresponding to peak to mean contrasts of 0.1, 0.3 and 0.7. All other experimental details (viewing distances, step size, randomization etc.) were identical to those in Expt 1.

Results

The results for Expt 2 are shown in Fig. 6. The data are again plotted in two different ways. In Fig. 6(A) the peak of the amplitude spectra (when the patterns were matched for apparent contrast) is plotted against the spatial frequency of the peak. In Fig. 6(B), the peak to mean contrast required for a perceptual match with the standard is plotted as a function of spatial frequency. All of the plotting conventions, including the use of different symbols, are as in Expt 1.

As with the filtered noise patterns, observers show approximate contrast constancy with these localized Gabor patches. The solid lines in Fig. 6(A) have a slope of -2 , indicating how the spectra peaks would fall in the case of perfect matches. As can be seen from the data, subjects adjusted the spectra of the Gabor functions to lower amplitude with increased spatial frequency. The slopes of the best fitting lines to the data were approx. -2.0 for all three contrast levels. In the isoresponse plots of Fig. 6(B), the data would fall along the solid lines in

the case of perfect matching. In these plots, departures from constancy are particularly evident at the lowest spatial frequencies tested, i.e. subjects show a clear decrease in relative sensitivity at 0.5 c/deg.

Note that none of the subjects made contrast matches beyond 16.0 c/deg. At 32.0 c/deg, the localized Gabor patches were reported to be either invisible or of higher contrast than the standard. Interestingly, similar reports were noted by Georgeson and Sullivan (1975) with respect to high frequency grating stimuli. At other points where matching was difficult or impossible, the test patch was reported to "fade rapidly from view" or to "appear as a single bright region" (i.e. the surround flanks of the Gabor were sometimes reported to disappear even though the center region was still seen as brighter than the background). As with the filtered noise patterns, the upper frequency at which contrast matching is possible decreases gradually with standard contrast.

Experiment 3—Contrast Matching as a Function of Contrast

The results of Expts 1 and 2 suggest that contrast matching is quite accurate as soon as the test or variable stimulus is above threshold, i.e. contrast constancy is observed soon after the stimulus becomes visible. In this experiment, we took a closer look at how subjects match contrast across the different scales as a function of contrast. In order to allow a more accurate assessment of the relative sensitivity profile at low and intermediate contrast levels, contrast matching was performed for six test frequencies over a range of 32 contrasts. As in Expt 2, matching was between pairs of Gabor patches using the method of adjustment. In this experiment, however, test frequencies ranged from 4 to 22.6 c/deg in half-octave steps, and the standard contrasts ranged from 1% to 97% (peak to mean contrast), spaced in a roughly logarithmic fashion. All frequencies were tested at a viewing distance of 3.8 m.

The methods differed in one important respect from those of Expts 1 and 2. In the current experiment, subjects adjusted the contrast of a 4 c/deg "variable" stimulus to match a "standard" stimulus which was set to a range of spatial frequencies and contrasts. Recall that in Expts 1 and 2, subjects adjusted the contrast of the various test stimuli to match the contrast of a 4 c/deg standard. This reversal in the choice of standard and variable stimulus was prompted by the difficulties experienced by subjects in matching high frequency stimuli at low contrast levels. In the earlier experiments, subjects reported that the high frequency stimuli changed abruptly from being invisible at low contrast levels to being of high apparent contrast at high physical contrasts, therefore making matching to a low contrast 4 c/deg standard impossible. Because sensitivity to spatial contrast peaks in the vicinity of 4 c/deg, it should be possible to match this stimulus to a high frequency stimulus of any contrast level. This method was also used by Kulikowski (1976).

Contrast adjustments to the 4 c/deg stimulus were made using the right and left workstation mouse buttons.

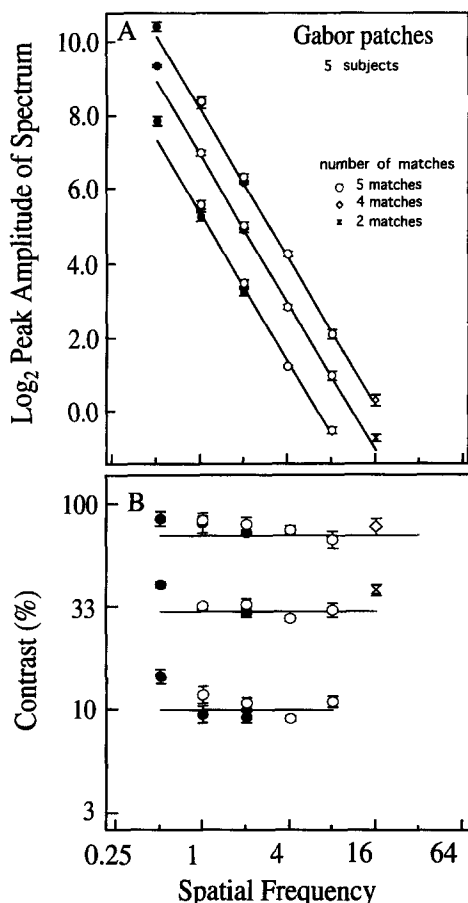


FIGURE 6. Contrast matching data for the Gabor patches (Expt 2) at three suprathreshold contrasts. The same data are plotted in two ways. In (A), the peak of the amplitude spectra (when the patterns were matched for apparent contrast) is plotted against the spatial frequency of the peak. In (B) the contrast required for a perceptual match with the standard is plotted as a function of spatial frequency. Subjects adjusted the contrast of the test frequency to match the contrast of the 4 c/deg standard. The solid symbols show results of the near condition while the open symbols show results for the far condition. Results were not included if the subjects stated that they could not make an acceptable match. The solid lines in both plots show predicted constancy.

When the standard stimuli were invisible, subjects were requested to convey this information by pressing the middle mouse button to make a zero contrast match.

As in the previous experiments, bit stealing was used to increase the range of luminance available on the display. For the 10 highest contrasts tested in this experiment (38–97%), the 8 bits were selected from the full 10-bit range. For the middle 10 levels (13–34%), the middle 60% of the full luminance range was used and for the 12 lowest contrasts (1–25%), the inner 25% of the range was used. On each matching trial, the standard stimulus was set to the appropriate contrast and the initial contrast of the variable stimulus was randomly set within limits. For each of the three contrast ranges, the variable was set within $\pm 25\%$ of the range average. The averages were 70%, 24% and 8% for the high, middle and low contrast ranges respectively. Two subjects each ran five experimental sessions (i.e. all frequencies at all contrasts). Sessions lasted an hour or more and were run on different days.

Results

The results of Expt 3 are shown separately for subjects NB and RD in Fig. 7(A, B) respectively. The matching contrast (i.e. the contrast to which the variable was set for a perceptual match) is plotted against the standard contrast for the four highest spatial frequencies tested. The matching contrasts were calculated by averaging the (log transformed) matches over the number of experimental sessions in which a non-zero match was made. Error bars indicate ± 1 SD about the means. As in the plots for Expts 1 and 2, different plot symbols are used to indicate the number of matches made at each data point. For example, the open circles indicate that matches were made in all five experimental sessions, the solid circles are used when matches were made on four out of five sessions, and so on (see legend). The solid triangles indicate contrasts at which the subject set the variable to zero contrast in all five sessions. A 45 deg line is included in each plot to show how the data would fall in the case of constancy.

Referring to subject NB, the first thing to note is that for all but the highest spatial frequency, there is a range of contrasts over which the data fall on the 45 deg line. Although contrast threshold varies markedly with spatial frequency, the matching curves have approximately the same slope once past threshold. In general, there appear to be three separate regions to the matching curves. Firstly, there is an initial region in which the test stimuli are subthreshold, as indicated by the zero contrast settings of the 4 c/deg variable stimulus. Secondly, the test stimuli are visible on some percentage of the trials in and around threshold. Matching is somewhat inaccurate in this region with the variable being set to both higher and lower contrasts than the standard. Finally, contrast is matched quite accurately over a region of relatively high contrasts, suggesting that contrast constancy holds once the patterns are clearly visible. At the highest spatial frequency tested (22.5 c/deg), subject NB shows evidence of a relatively lower sensitivity over almost the entire

contrast range tested. The 4 c/deg variable stimulus was consistently set to a lower contrast than the standard for a perceptual match.

Most of these observations can also be made for subject RD. His thresholds appear to be somewhat higher at all frequencies, especially at 22.5 c/deg where few non-zero matches were made. The boundaries between suprathreshold and subthreshold contrast are again marked by both overestimation and underestimation of contrast and by an increase in the number of zero contrast matches.

Both subjects showed accurate matching over almost the entire range of contrasts at the two lowest frequencies tested (4 and 5.5 c/deg). The data for these frequencies are not shown.

DISCUSSION

The results of Expts 1 and 2 show that contrast constancy is maintained over a range of scales for the filtered noise patterns and Gabor patches. The results of Expt 3 suggest that contrast constancy occurs almost as soon as the stimuli are suprathreshold, and this appears to be the case for all but the highest spatial frequency tested. Contrast thresholds do increase with spatial frequency for these bandpass stimuli, but once past threshold, the matching curves have approximately the same slope at all spatial frequencies. This suggests that the underlying contrast–response function of the system (whatever its exact shape or form) is similar across scale, except for a difference in threshold. We will return to this issue later. First, we would like to discuss two models which can handle these suprathreshold results.

Modeling

As a first step toward understanding the basis of contrast constancy, it is useful to note that the peak-to-trough contrast is roughly constant when the patterns are matched in contrast. This holds for the various different patterns for which constancy has been demonstrated, i.e. sinusoidal gratings, Gabor patches and filtered noise patterns. By comparison, it is clearly not possible to determine which functions will appear equal in contrast by considering amplitude spectra alone, because the spectra of these different functions scale in quite different ways. Sinusoidal gratings are matched when their spectra are roughly constant in amplitude (Georgeson & Sullivan, 1975). However, the Gabor patches are matched in contrast when the peaks of the amplitude spectra fall as $1/f^2$ and the noise patterns are matched when the spectral peaks fall as $1/f$.

The problem then is to describe a model which provides a constant response when the peak to trough contrast of a pattern is constant across scale. This is relatively straightforward in the case of a single-channel model. However, in order to explain constancy for these diverse patterns in terms of a multi-channel model, a particular relationship between the bandwidth and peak sensitivity of individual mechanisms is required.

Single-channel model. One approach to explaining the experimental data is to presume that contrast matching is mediated by a single broadband channel. First consider the Gabor patches. These patterns are matched in apparent contrast when roughly equal in peak luminance or contrast. A broadband mechanism (i.e. an impulse response) which reads the luminance of the peak will show constancy across scale. In the case of the random phase stimuli, the waveforms are matched in apparent contrast when their variance or r.m.s. contrast are roughly constant. Again, a broadband mechanism which reads the average deviation from the mean luminance across the image will show constancy. If such a broadband mechanism underlies contrast constancy, then the results of the current experiments and those of previous investigators (e.g. Georgeson & Sullivan, 1975) suggest that this mechanism must have a relatively flat spectral response out to frequencies of around 16–32 c/deg.

Interestingly, the results of a number of suprathreshold studies using noise stimuli provide support for a model in which contrast energy is integrated across a broad band of frequencies. For example, the r.m.s. contrast thresholds for the suprathreshold detection of noise reported by Kersten (1987) are consistent with an energy detection model. In this study, high efficiency (or

performance relative to the “ideal” detector) was roughly constant over a 2–6 octave band range, suggesting a channel with broad frequency bandwidth. Likewise, Quick, Hamerly and Reichert (1976) and Jamar and Koenderink (1985) report no measurable critical band in their suprathreshold data.

Both physiology and psychophysics provide evidence for the existence of multiple spatial frequency channels tuned to different frequencies. This suggests two ways in which these relatively broadband results may be interpreted. First, the broadband data may reflect pooling among multiple channels such that the system behaves like a single broadband mechanism. Along this line, the authors cited above have considered how the outputs of different channels might be combined or pooled to account for their results. Secondly, cortical cells show a range of frequency bandwidths (Tolhurst & Thompson, 1981). Thus the visual system may employ the bandwidth best suited to the stimulus. By this hypothesis, narrow-band stimuli are processed by relatively narrow-band mechanisms and broadband stimuli are processed by relatively broadband mechanisms.

By either approach, one would assume that the stimuli used in the current studies are processed by multiple channels tuned to different frequencies. If this is the case,

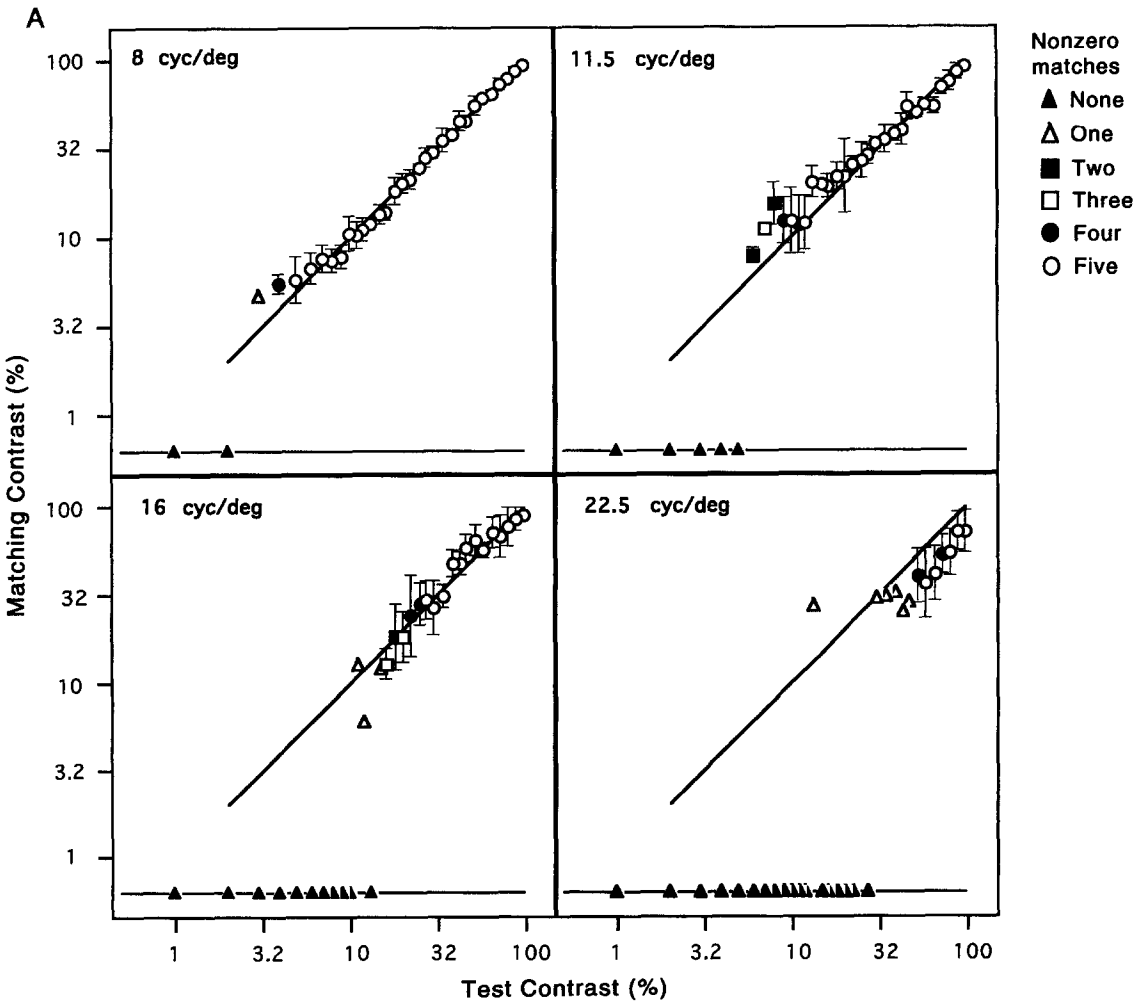


Fig. 7—Caption of facing page.

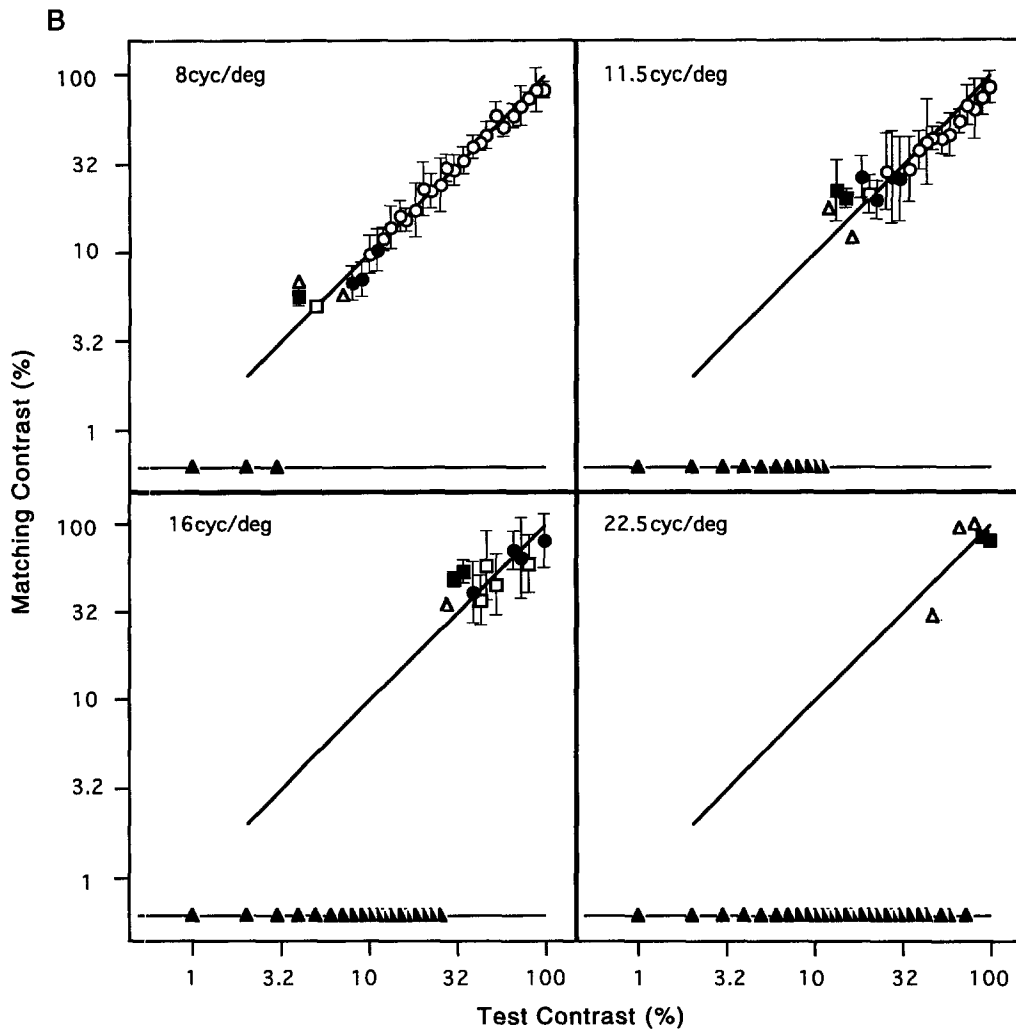


FIGURE 7. Contrast matching data for the Gabor patches over a large range of standard contrasts (Expt 3). Results are shown separately for (A) subject NB and (B) subject RD. Unlike Expts 1 and 2, subjects adjusted the contrast of the 4 c/deg standard to match the contrast of the test. The matching contrast of the standard is plotted against the test contrast for the four highest spatial frequencies tested in this experiment (8.0, 11.5, 16.0 and 22.5 c/deg). Zero contrast is indicated by the dotted lines in each plot. The results suggest that the apparent contrast of each stimulus is relatively accurate as soon as it is above threshold. See text for details.

then our data provide an opportunity to explore the relative sensitivity of these channels. In the following section we make the assumption that each pattern is processed by mechanisms tuned to the central spatial frequency of the stimulus. To account for our results, these channels must have a rather specific sensitivity profile.

Multi-channel model. Both psychophysical and physiological research supports the theory that spatial patterns are represented by arrays of cells tuned to different frequencies. At the level of threshold sensitivity, it has been shown that detection of complex gratings is in accordance with multi-channel rather than single-channel model predictions (Campbell & Robson, 1968; Graham & Nachmias, 1971; Sachs, Nachmias & Robson, 1971). At suprathreshold levels also, tasks requiring the detection of narrow-band stimuli often provide clear evidence for the operation of independent frequency channels, e.g. masking of grating patterns by noise suggests a critical band of about ± 1 octave (Stromeyer & Julesz, 1972). To a first approximation, the psychophysically defined

channels have linear bandwidths which increases in proportion to frequency, so that they are approximately constant on a log frequency axis. Neurophysiological studies likewise report that the frequency bandwidths of cortical cells increase with peak tuning. DeValois, Albrecht and Thorell (1982) report a median bandwidth of 1.4 octaves for macaque simple cells, although octave bandwidths appear to decrease somewhat at higher spatial frequencies.

If we assume that such bandpass mechanisms underlie the contrast matching data, what do these data suggest about the sensitivity of these mechanisms? How should we model the relative sensitivity of the different frequency selective mechanisms? Figure 8 shows an example of a multi-channel model which can account for the matching results. In this model, all of the frequency selective mechanisms have the same peak sensitivity while the bandwidth increases in proportion to frequency. This sensitivity distribution was previously proposed by Field (1987) because it provided a distributed response to natural scenes. As was noted, if the peak sensitivity is

constant and the bandwidths increase with frequency, then images with $1/f$ amplitude spectra (natural scenes) will on average produce the same response throughout the array of frequency selective mechanisms. This basic model is also implied in the work of Kingdom and Moulden (1992).

Two assumptions are made regarding how contrast is mediated by the spatially localized filters of the multi-channel model. In the case of the Gabor patches, it is assumed that perceived contrast is determined by the output of a filter which is centered on the patch and is matched to it in scale. In the case of the bandpass noise patterns, it is assumed that contrast is determined by the average contrast-response of filters distributed across the image, also matched in scale to the pattern. This approach to modeling the contrast-response in the two tasks is outlined in Fig. 9. It should be noted that this general approach is not new to this study. Similar assumptions have been made to account for the detection of grating patches in noise (Kersten, 1984) and the suprathreshold detection of broadband noise (Kersten, 1987). It should also be noted that the model does not involve response pooling across cells tuned to different frequencies for either stimulus.

The following terminology is used to describe how the filters change with scale; $h(x, y)$ is used to represent a two-dimensional filter in space, $H(u, v)$ is its spectrum and a is a scale factor. As the filters become more localized in space, their peak spatial sensitivity increases so that the total volume under the filters is kept constant. By the properties of the Fourier transform discussed above [equation (4)], the peak sensitivity in frequency

remains constant across scale under these conditions. As depicted in Fig. 8, the scaling properties of the proposed filters can be summarized in either the spatial (left side) or the frequency domain (right side) as follows

$$a^2 h(ax, ay) \Leftrightarrow H(u/a, v/a). \quad (6)$$

Note how the peak response in space increases by a factor of a^2 as the spatial extent of the mechanism decreases by a factor of a in both dimensions. In the Fourier domain, the frequency response remains constant as the spectral extent increases. A proof of how such mechanisms give a contrast response across scale to both the Gabor functions and the noise patterns is given here.

Coherent patterns. The case of the Gabor patterns is considered first. These scaled patterns appeared matched in contrast when they were roughly equal in physical contrast. In this case, the peaks of the amplitude spectra fall in proportion to the square of frequency. As shown in Fig. 4(A), the scaling of the stimuli can be summarized as

$$g(ax, ay) \Leftrightarrow a^{-2} G(u/a, v/a). \quad (7)$$

Assuming that the perceived contrast is mediated by the activity of a matched filter centered on the Gabor patch, we can determine how the model behaves across scale by cross-correlating the filter with the spatial profile of the patch (see Fig. 9, left side). From equations (6) and (7), the output of the centered filter is

$$R = a^2 \iint h(ax, ay) g(ax, ay) dx dy. \quad (8)$$

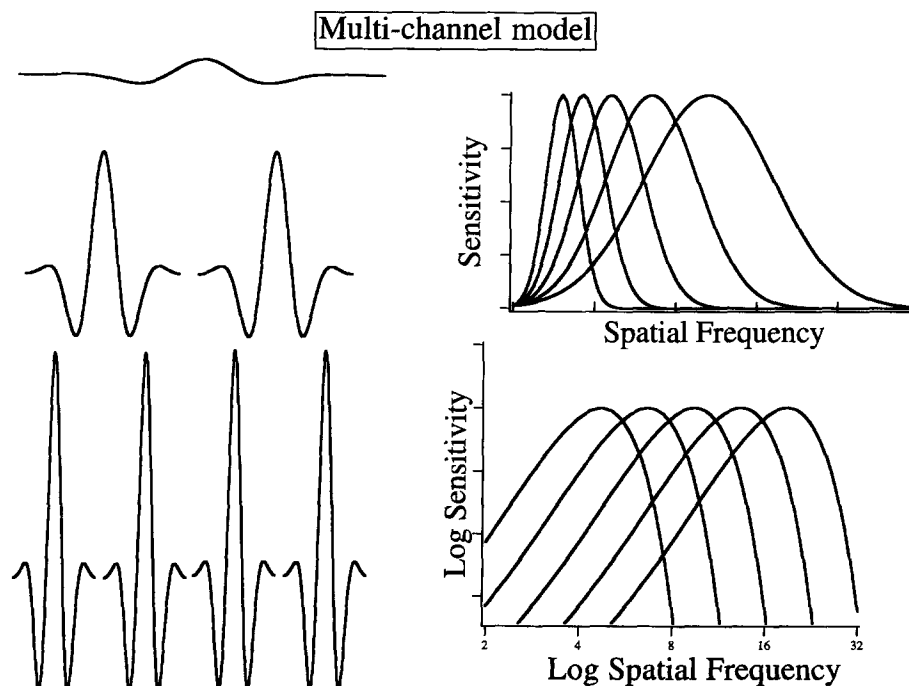


FIGURE 8. The proposed multi-channel model. For convenience, one-dimensional mechanisms are shown here, so that the peak spatial sensitivity of the filters increase in proportion to frequency. For two-dimensional mechanisms, the increase in peak spatial sensitivity would be proportional to the square of frequency and the spectra plots would represent one-dimensional slices through the two-dimensional spectra. The model also assumes that the contrast-response functions are the same across spatial frequency.

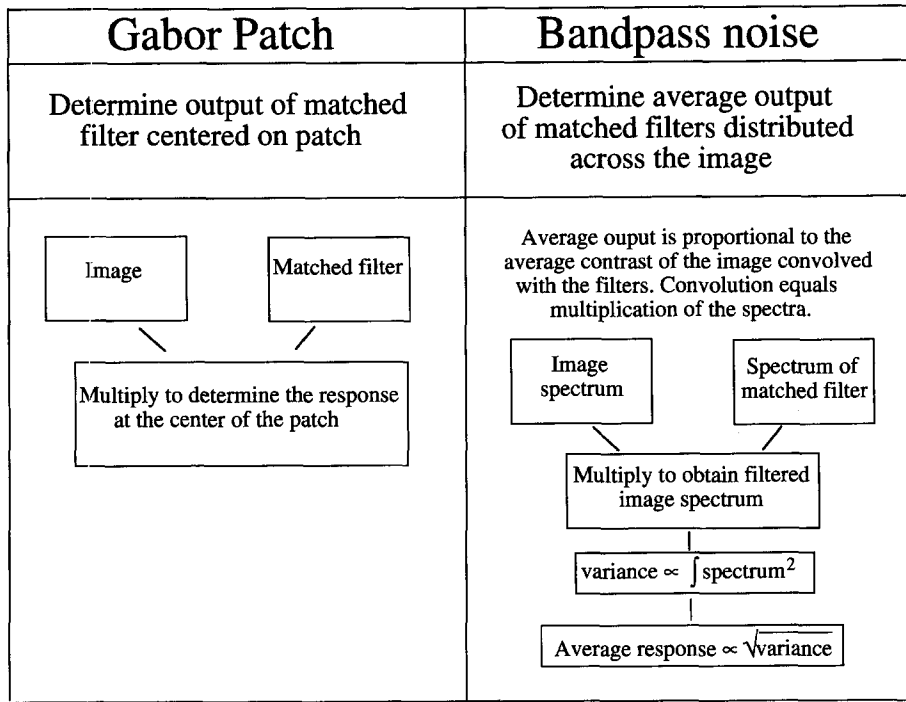


FIGURE 9. A summary of the model assumptions. For the Gabor patches, we assume that perceived contrast is mediated by the response of a filter centered on the patch. For the bandpass noise stimuli, we assume that perceived contrast is determined by the average outputs of cells distributed across the image. In the case of the noise patterns, we calculate this average response in terms of the variance of the image after convolution. This method of calculating the average response or a cell array is mathematically convenient. However, we do not presume that the visual system calculates its average response using this frequency domain technique. The model also assumes that the contrast-response functions do not change with increasing frequency.

Letting $\alpha = ax$ and $\beta = ay$, and using the change of variables theorem,

$$R = a^2 \iint h(\alpha, \beta) g(\alpha, \beta) \frac{1}{a^2} d\alpha d\beta. \quad (9)$$

Since the scale factor a cancels, the filter output, R , is constant across scale.

This constant response across scale is assumed to underlie the perceptual phenomenon of contrast constancy for the Gabor patches. It is important to note that the response to these patterns remains constant only when the model mechanisms have the characteristics described in equation (6) and shown in Fig. 8.

Incoherent patterns. In the case of the filtered noise, perceived contrast is also assumed to be mediated by the response of mechanisms which are tuned to the range of spatial frequencies in the pattern. However, here it is the average response of mechanisms distributed across the image which is of interest (see Fig. 9, right side). In order to calculate this average response, the image is firstly convolved with a filter of matched scale. By Fourier theory, the convolution of an image and a filter is equivalent to the multiplication of their spectra in the frequency domain. For convenience, the proof is made in the frequency domain.

The bandpass noise patterns were matched in perceived contrast when they had roughly equal variance or r.m.s. contrast. In this case, the peaks of amplitude spectra fall in proportion to frequency

as the patterns scale. The scaling of the spectra is summarized as

$$a^{-1}G(u/a, v/a). \quad (10)$$

From equations (6) and (10), the spectrum of the image after convolution with the filters is

$$a^{-1}G(u/a, v/a)H(u/a, v/a). \quad (11)$$

As noted above [equation (3)], the variance of an image is proportional to the integral of its power spectrum. Therefore, from equation (11)

$$\text{Var} = \iint [a^{-1}G(u/a, v/a)H(u/a, v/a)]^2 du dv. \quad (12)$$

Letting $\alpha = u/a$ and $\beta = v/a$, and using the change of variables theorem

$$\text{Var} = a^{-2} \iint [G(\alpha, \beta)H(\alpha, \beta)]^2 a^2 d\alpha d\beta. \quad (13)$$

Again, the scale factor a cancels. Since the average response of the filters is simply the square root of the variance,

$$R_{\text{avg}} = \sqrt{\text{Var}}$$

this average response is constant across scale, and contrast constancy is thus predicted for the noise patterns. Again, what is important is that the scaling of sensitivity in the multi-channel model must follow that described in

equation (6) and portrayed in Fig. 8 in order to account for constancy for these patterns.

In summary, the multi-channel model shown in Fig. 8 predicts constancy for both types of pattern, assuming that perceived contrast is mediated by a cell centered on the stimulus in the case of the Gabor functions, and by the average response of cells distributed across the image in the case of the noise patterns. It may appear that this model also assumes that the contrast-response functions of the individual mechanisms are linear. This is not the case. We have described the conditions under which filters tuned to different spatial frequencies produce the same response. Applying an output nonlinearity of the same form at each spatial frequency will not change the constancy of the response across scale. To conclude, as long as the cells at different scales have the same contrast-response function (linear or nonlinear), the model predicts a constant output to the scaled stimuli used in the experiments.

GENERAL DISCUSSION

Previous studies have demonstrated contrast constancy for high contrast sinusoidal gratings (e.g. Georgeson & Sullivan, 1975; Kulikowski, 1976; Watanabe *et al.*, 1968). Our results show that almost as soon as these stimuli are visible, contrast constancy holds for bandpass noise patterns and scaled Gabor functions. We have described a multi-channel model which can account for contrast constancy to all three types of stimuli. The model assumes that the peak contrast sensitivity of the underlying channels is constant across frequency and assumes that the contrast-response functions have the same "slope" across spatial frequency.

However, some departures from constancy were noted in the experimental data, at both the lowest and the highest spatial frequencies tested. For example, at 0.5 c/deg (Expt 2) and at 25.6 c/deg (Expt 3) observers showed a lower relative sensitivity to contrast. How might these departures from constancy be explained in terms of the model? One possible reason is that the highest and lowest frequency stimuli may be processed by channels whose optimal frequency is not matched to the central frequency of the pattern. There appear to be both upper and lower limits on the peak frequency tuning of cells or channels. For example, DeValois *et al.* (1982) report that the peak tuning of macaque cortical cells falls between 0.5 and 15 c/deg. Similarly, an adaptation study by Blakemore and Campbell (1969) suggests a lower limit to the peak tuning of frequency channels of around 3 c/deg. So for example, it may be that the visual response to the 25.6 c/deg pattern is determined by a channel whose optimal frequency is lower than this. Under these circumstances, the observed departures from constancy would be expected.

One important question about the model proposed here is to what extent it is supported by physiological data. As noted earlier, physiological results are consistent with the general notion of a multi-channel representation of contrast information at early cortical stages. Regarding

frequency bandwidths, mammalian cortical simple cells have spatial frequency bandwidths which increase with peak frequency, although octave bandwidths do decrease somewhat with frequency (DeValois *et al.*, 1982; Tolhurst & Thompson, 1981). Physiological data on the absolute peak sensitivity of cells tuned to different frequencies is harder to come by, presumably because noisy data are usually normalized. However, a recent study by Croner and Kaplan (1995) shows that for ganglion cells of the primate, the relation between receptive field size and peak response is roughly described by equation (6). Their results, as well as previous psychophysical results (e.g. Georgeson & Sullivan, 1975), and the data of this paper can be interpreted as support for the notion that mechanisms tuned to different frequencies have equal peak spectral sensitivity.

The model presented in this paper differs in two important respects from a number of other models of suprathreshold contrast processing. Firstly, the model does not include a "response pooling" stage as is typical in many other models (e.g. Cannon & Fullenkamp, 1988; Swanson, Wilson & Giese, 1984). That is, we have made no assumptions about how the responses of channels tuned to different frequencies might be combined or summed. The stimuli used in the current studies all had a frequency bandwidth of about 1.6 octaves, which is within the range of cortical cell bandwidths. While response pooling may be an important consideration when using stimuli with broader frequency bandwidths, we have not found it necessary to incorporate it here.

Secondly, a number of investigators have suggested that channels tuned to higher frequencies have a higher response gain (or "steeper" contrast-response function) than those tuned to lower spatial frequencies. In some instances, the difference between threshold sensitivity and suprathreshold constancy has been explained in terms of this increase in gain with spatial frequency (e.g. Georgeson & Sullivan, 1975; Swanson *et al.*, 1984). Response gain is not assumed to increase with spatial frequency in our model. Rather, it is implicitly assumed that the contrast-response functions have the same shape or form across channels tuned to different frequencies, and in fact this is what is suggested by the contrast matching data from Expt 3. These data do not allow estimates of the actual shape of the contrast-response functions, but are consistent with a number of monotonic contrast-response functions, including the nonlinear form estimated for individual cortical cells (e.g. Albrecht & Hamilton, 1982).

However, there remains the question as to why a system which shows constancy at suprathreshold contrasts has a threshold profile in which sensitivity varies with spatial frequency (i.e. the CSF). The fall-off in threshold sensitivity to spatial contrast at high frequencies has been attributed both to optical blurring and to "neural attenuation" of contrast, with post optical factors playing the larger role (Campbell & Green, 1965). A number of studies have attempted to account for the differences between threshold detection data and suprathreshold matching results (e.g. Georgeson & Sullivan, 1975;

Swanson *et al.*, 1984; Swanson, Georgeson & Wilson, 1988). Here we consider three different explanations for the observed changes in sensitivity.

Differences in gain across spatial frequency

One suggestion is that the frequency dependent differences in contrast sensitivity which are observed behaviorally reflect a difference in the sensitivity of the underlying cells or channels. Georgeson and Sullivan (1975) proposed that these differences are corrected for at suprathreshold levels by some form of gain adjustment. Specifically, the proposal was that channels tuned to higher frequencies have a greater response gain, thereby "deblurring" the signal at high contrasts. Indeed, several investigators have suggested that channels tuned to high frequencies have both higher thresholds and "steeper" contrast-response (or "transducer") functions (e.g. Swanson *et al.*, 1984, 1988). According to this type of model, contrast matching between a high frequency test stimulus and a medium frequency standard should be inaccurate over some range of low and intermediate suprathreshold contrasts before contrast constancy is observed. Our relative sensitivity to the high frequency stimulus should be quite poor at low contrast settings of the standard. But because the gain of the high frequency mechanism is assumed to be higher, this difference in sensitivity (as measured by matching) should decrease gradually with increased contrast of the standard, until constancy is observed.

Our contrast matching data do not support this notion. Consider again the data from Expt 3 (Fig. 7). As is expected from numerous other studies, contrast thresholds increase with spatial frequency so that contrast sensitivity is lower for the high spatial frequency Gabors. It is important to note that at high frequencies, our data show no evidence of a gradual shift in perceived contrast from low perceived contrast near threshold to high perceived contrast. Rather, the Gabor stimuli are matched quite accurately almost as soon as they first become visible, so that the transition between the subthreshold region and the region of suprathreshold constancy is quite abrupt. We will return to this point.

A psychophysical linking hypothesis

A second approach is to assume that perceived contrast is not a simple linear function of a channel's output. For example, one might presume that contrast constancy is dependent on experience with stimuli as they vary in size and that the relation between a cell's activity and the contrast it represents is learned. Perhaps threshold data reflect actual differences in physiological sensitivity while matching data describe the learned response between perceived contrast and response magnitude. In this case,

the perceived contrast of a stimulus will not tell us much about the sensitivity of the underlying mechanisms. Our data do not allow us to disprove this "psychophysical" linking hypothesis. However, there is another explanation which we believe can handle our suprathreshold data as well as predict the increase in thresholds with increasing spatial frequency.

Equal peak gain across spatial frequency but unequal noise

A third possibility is that the differences in threshold sensitivity are due in large part to frequency dependent differences in noise. Here we assume that the contrast-response functions have the same form at different spatial frequencies, i.e. the responses of different channels to gratings of their optimal spatial frequency are the same at each contrast level.* In the model described earlier (Fig. 8), the peak sensitivity of the different channels is constant across frequency, but the linear bandwidths increase with frequency (i.e. integrate over a wider region of the spectrum). This means that the higher frequency cells will produce a larger response to flat spectrum or white noise than the low frequency cells. Because the response to gratings is constant across frequency while the response to noise increases with frequency, the signal-to-noise ratio decreases with increasing spatial frequency. Assuming that detection is limited by such noise, we would expect contrast thresholds to increase with increasing frequency. It has been suggested that photon noise, which has a flat spectrum, is a determining factor in threshold responses (e.g. Banks, Geisler & Bennett, 1987; Atick & Redlich, 1992). Whatever the source of the noise, if its effective spectrum is flat, then thresholds are expected to increase according to our model even though the contrast-response functions are the same at different frequencies.

Our matching data are compatible with this type of model. As shown in Fig. 7, contrast thresholds increase with spatial frequency as expected if thresholds are determined by noise. The constancy observed at suprathreshold levels is also expected, given the assumption of equal "response gain" at different spatial frequencies. If the contrast-response functions have the same form across frequency, then the contrast matching curves (as plotted in Fig. 7) should have a slope of 1.0 at all spatial frequencies. Although the data are somewhat noisy at the highest frequencies, all of the suprathreshold results fall near this line.

These results appear to differ from those of previous investigators. For example, the results of matching studies with grating stimuli (Georgeson & Sullivan, 1975) and with broadband stimuli (Swanson *et al.*, 1984; Cannon & Fullenkamp, 1991a) appear to suggest that the matching curves should show a smooth transition between threshold contrast and the contrast at which constancy is observed. By comparison, our data show this transition to be quite abrupt. Poirson and Wandell (1993) recently replotted the data of Georgeson and Sullivan (1975) and showed that above 5% contrast, the matching is quite accurate. Poirson and Wandell's own data from

*In assuming that the contrast-response functions are the same at different spatial frequencies, we do not preclude the possibility that the response gain of a channel changes as a function of contrast, i.e. the contrast-response functions may be nonlinear. All that is required is that they have the same form at different spatial frequencies.

contrast matching with chromatic gratings also show accurate matching down to relatively low contrasts.

Our data show no evidence for a transitional region even at low contrasts. This difference is probably due in part to differences in methodology. First, our subjects (in Expt 3) adjusted the contrast of a 4 c/deg stimulus to match the contrast of a range of test frequencies of higher spatial frequency. Many matching studies have used the reverse method of adjusting the contrast of a high spatial frequency pattern to match a 4 or 5 c/deg standard. As noted earlier, subjects may have no choice but to increase the contrast of the test stimulus in order to make it visible, at which point it may have a higher perceived contrast than a low contrast standard.

Secondly, in Fig. 7 we have plotted matches only when the subjects were capable of making an acceptable match. Near threshold, subjects could sometimes make matches (the high spatial frequency pattern appeared to be high contrast) and sometimes could not see anything (zero contrast). If we had averaged these two (matches to zero contrast and matches to high contrast), the transition between threshold contrast and the contrast at which constancy is observed would appear more gradual.

To summarize, threshold sensitivity is assumed to be a function of the signal to noise ratio (e.g. Watson, 1992), whereas perceived contrast is assumed to be a function of the signal alone and to be independent of the noise. Our model predicts a decrease in contrast sensitivity with spatial frequency, because the system's response to noise increases with frequency. However, perceived contrast at suprathreshold levels is assumed to be determined by the signal strength alone, and this is constant across frequency. Thus, the model predicts both contrast

constancy at suprathreshold contrasts and increased contrast thresholds with increasing frequency without the need to hypothesize changes in the gain of cells across frequency. Since there appears to be no physiological evidence for such a change in gain (e.g. Dean, 1981), and since our approach can handle both threshold and suprathreshold data, we believe that our approach provides a more parsimonious explanation of the data.

We do not mean to suggest that this model can account for all existing data regarding the perception of suprathreshold contrasts. Lateral inhibitory effects (e.g. "contrast-contrast") such as those described by Chubb, Sperling and Solomon (1989) and Cannon and Fullenkamp (1991b), certainly require a more detailed model than that discussed here. Furthermore, stimuli with bandwidths greater than 2 octaves may require considerations of response pooling. Various researchers have used some form of response pooling to account for broadband data (e.g. Swanson *et al.*, 1984; Cannon & Fullenkamp, 1991a,b; Quick *et al.*, 1976). For our stimuli, such complexities do not appear to be required.

One central component of our model which differs from previous accounts is that we have not found it necessary to assume that the contrast-response gain of the channels varies as a function of frequency. Instead, we assume that the peak response is constant across frequency even at threshold. According to our model, the fall-off in contrast sensitivity at high frequencies does not reflect a fall-off in the peak response of the underlying channels. Rather, it reflects the amount of effective noise in the system. The fact that this noise is not visible at suprathreshold

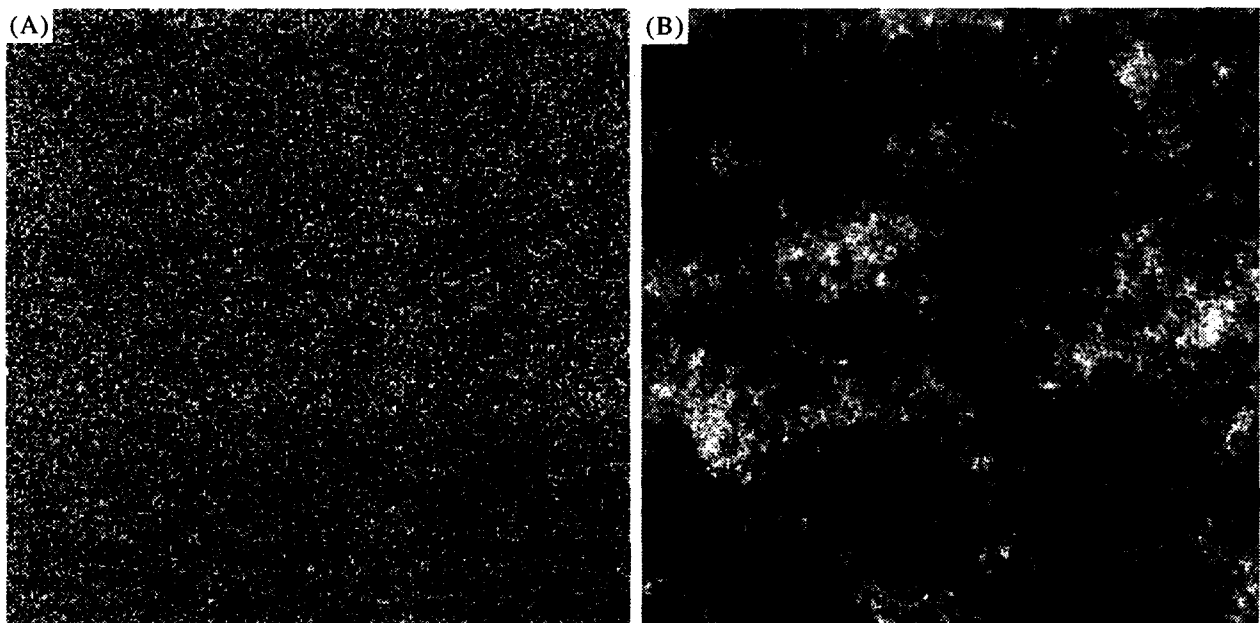


FIGURE 10. A white noise pattern (A) and a white noise pattern filtered to a spectrum of $1/f$ (B). The multi-channel model presented here predicts that the response to a white noise pattern will increase out to somewhere between 16 and 32 c/deg while the response to the $1/f$ pattern will be approximately constant over the same frequency range. Indeed, the reader will probably notice that the white noise pattern appears to be dominated by high frequency structure while the $1/f$ pattern appears to have structure at a variety of scales.

contrasts suggests that it is somehow removed by later processing. This is an area we are currently exploring. A broadly tuned contrast gain control mechanism, such as modeled by Heeger (1992), may play a role in this process.

Sensitivity to natural scenes

Another advantage of this model is that it predicts a constant-response at different scales to images with $1/f$ spectra like those found with natural scenes. Consider the two images shown in Fig. 10. On the left is a white noise pattern. The reader will probably notice that the white noise pattern appears to be dominated by high frequency structure while the $1/f$ pattern appears to have structure at a variety of scales. As noted earlier, one problem with more traditional measures of sensitivity concerns their inability to predict perception of contrast in broadband scenes. In this case, knowledge that sensitivity to high contrast gratings is roughly constant across some range of frequencies does not predict the difference in perception for these two patterns. By comparison, the multi-channel model in Fig. 8 does. Because this model considers how the channels integrate across frequency, the model predicts that the response to a white noise pattern will increase with frequency whereas the response to a $1/f$ pattern should be constant over that same range.*

Finally, a comment should be made regarding the "failure" of linear systems analysis. As noted in the Introduction to this paper, the contrast sensitivity function and the suprathreshold matching function for gratings often fail to predict the visual response to broadband patterns. One reason for this failure is that these functions do not describe the extent to which mechanisms integrate information across space or frequency. Because threshold sensitivity to contrast peaks around 4 c/deg, one might conclude that we would see suprathreshold stimuli best in this region. However, because cells at high frequencies have broader linear bandwidths, this measure of sensitivity fails to predict the response to broadband patterns.

An alternative description of how the visual response to contrast changes across scale is clearly required to deal with broadband patterns. One approach is to describe the "sensitivity" of a cell in a way which incorporates both its peak response and its bandwidth into a single metric. For example, each cell may be described as a vector and the visual transform may be treated as a rotation of the coordinate system (Field, 1994). The integrated response or broadband sensitivity of a cell is then given by the vector length. In the frequency domain, this means that the integrated response is proportional to the square root of the volume under the power spectrum. In the model depicted in Fig. 8, vector length will increase

in proportion to spatial frequency. Our experimental results show that contrast constancy holds out to approximately 20 cycles/deg. In terms of our model, these data suggest that the integrated response of the underlying cells is largest around 20 c/deg. We discuss this approach at length in another paper (Field & Brady, 1995). However, it should be stressed that the optimal description of sensitivity is not likely to be the peak threshold response to a sinusoidal grating.

CONCLUSIONS

In this paper we have discussed a model of broadband sensitivity to contrast which can account for contrast constancy under the various conditions in which it holds. Previous research in this area has shown that constancy holds at high contrast for sinusoidal gratings (e.g. Georgeson & Sullivan, 1975) and we have shown constancy to also hold for relatively broadband patterns viewed at suprathreshold contrasts. These include Gabor patches (coherent phase) and bandpass noise patterns (random phase).

We suggest that a particular multi-channel model can account for all of these results. In this model, frequency tuned mechanisms are assumed to have equal peak spatial frequency sensitivity and octave constant bands. Although no assumptions have been made with regards to the precise form of the contrast-response functions, we assume that the contrast response to sinusoidal gratings shows almost no change across spatial frequency. We have shown how this model can account for our contrast matching results, and we suggest that this sensitivity profile makes sense ecologically given the statistics of natural scenes.

REFERENCES

- Albrecht, D. G. & Hamilton, D. B. (1982). Striate cortex of monkey and cat: contrast response function. *Journal of Neurophysiology* 48(1), 217-237.
- Atick, J. J. & Redlich, A. N. (1992). What does the retina know about natural scenes? *Neural Computation*, 4, 449-572.
- Banks, M. S., Geisler, W. S. & Bennett, P. J. (1987). The physical limits of grating visibility. *Vision Research*, 27, 1915-1924.
- Blakemore, C. B. & Campbell, F. W. (1969). On the existence of neurons in the human visual system selectively sensitive to the orientation and size of retinal images. *Journal of Physiology*, 203, 237-260.
- Blakemore, C. B., Muncey, J. P. J. & Ridley, R. M. (1973). Stimulus specificity in the human visual system. *Vision Research*, 13, 1915-1931.
- Bracewell, R. N. (1986). *The Fourier transform and its applications* (2nd edn). New York: McGraw-Hill.
- Burton, G. J. & Moorhead, I. R. (1987). Color and spatial structure in natural scenes. *Applied Optics*, 26, 157-170.
- Campbell, F. W. & Green, D. G. (1965). Optical and retinal factors affecting visual resolution. *Journal of Physiology*, 181, 576-593.
- Campbell, F. W. & Robson, J. G. (1968). Application of fourier analysis to the visibility of gratings. *Journal of Physiology*, 197, 551-566.
- Cannon, M. W. & Fullenkamp, S. C. (1988). Perceived contrast and stimulus size: experiment and simulation. *Vision Research*, 28, 695-709.
- Cannon, M. W. & Fullenkamp, S. C. (1991a). A transducer model for contrast perception. *Visual Research*, 31, 983-998.

*Obviously, there will be a limit to the frequency range over which the integrated response increases. For example, our contrast matching data suggest that the integrated response begins to fall off somewhere between 16 and 32 c/deg.

- Cannon, M. W. & Fullenkamp, S. C. (1991b). Spatial interactions in apparent contrast: Inhibitory effects among grating patterns of different spatial frequencies, spatial positions and orientations. *Vision Research*, 31, 1985–1998.
- Chubb, C., Sperling, G. & Solomon, J. A. (1989). Texture interactions determine perceived contrast. *Proceedings of the National Academy of Sciences U.S.A.*, 86, 9631–9635.
- Croner, L. J. & Kaplan, E. (1995). Receptive fields of P and M ganglion cells across the primate retina. *Vision Research*, 35, 7–24.
- Daly, S. (1989). Application of a noise adaptive contrast sensitivity function to image data compression. Human vision, visual processing and digital display. *SPIE*, 1077.
- Dean, A. F. (1981). The relationship between response amplitude and contrast for cat striate cortical neurones. *Journal of Physiology*, 318, 413–427.
- DeValois, R. L., Albrecht, D. C. & Thorell, L. G. (1982). Spatial frequency selectivity of cells in macaque visual cortex. *Vision Research*, 22, 545–559.
- Field, D. J. (1987). Relations between the statistics of natural images & the response properties of cortical cells. *Journal of the Optical Society of America A*, 4, 2379–2394.
- Field, D. J. (1993). Scale-invariance and self-similar 'wavelet' transforms: An analysis of natural scenes and mammalian visual systems. In Farge, M., Hunt, J. & Vassilicos (Eds), *Wavelets, fractals and Fourier transforms*. Oxford: Oxford University Press.
- Field, D. J. (1994). What is the goal of sensory coding? *Neural Computation*, 6, 559–601.
- Field, D.J. & Brady, N. (1995). Where is the peak of visual sensitivity? In preparation.
- Georgeson, M. A. & Sullivan, G. D. (1975). Contrast constancy: deblurring in human vision by spatial frequency channels. *Journal of Physiology*, 252, 627–656.
- Graham, N. & Nachmias, J. (1971). Detecting of grating patterns containing two spatial frequencies: A comparison of single and multiple channel models. *Vision Research*, 17, 637–652.
- Heeger, D. J. (1992). Normalization of cell responses in cat striate cortex. *Visual Neuroscience*, 9, 181–197.
- Jamar, J. H. T. & Koenderink, J. J. (1985). Contrast detection and detection of contrast modulation for noise gratings. *Vision Research*, 25, 511–521.
- Kersten, D. (1984). Spatial summation in visual noise. *Vision Research*, 24, 1977–1990.
- Kersten, D. (1987). Statistical efficiency for the detection of visual noise. *Vision Research*, 27, 1029–1040.
- Kingdom, F. & Moulden, B. (1992). A multi-channel approach to brightness coding. *Vision Research*, 32, 1565–1582.
- Kulikowski, J. J. (1976). Effective contrast constancy and linearity of contrast sensation. *Vision Research*, 16, 141–143.
- Poirson, A. B. & Wandell, B. A. (1993). Appearance of colored patterns: Pattern-color separability. *Journal of the Optical Society of America*, 10, 2458–2470.
- Quick, R. F., Hamerly, J. R. & Reichert, T. A. (1976). The absence of a measurable 'critical band' at low suprathreshold contrasts. *Vision Research*, 16, 351–355.
- Sachs, M. B., Nachmias, J. & Robson, J. G. (1971). Spatial frequency channels in human vision. *Journal of the Optical Society of America*, 61, 1176–1186.
- Stromeyer, C. F. & Julesz, B. (1972). Spatial-frequency masking in vision: Critical bands and spread of masking. *Journal of the Optical Society of America*, 62, 1221–1232.
- Swanson, W. H., Georgeson, M. A. & Wilson, H. R. (1988). Comparison of contrast responses across spatial mechanisms. *Vision Research*, 28, 457–459.
- Swanson, W. H., Wilson, H. R. & Giese, S. C. (1984). Contrast matching data predicted form increment thresholds. *Vision Research*, 24, 63–75.
- Tolhurst, D. J. & Thompson, I. D. (1981). On the variety of spatial frequency selectivities shown by neurones in area 17 of the cat. *Proceedings of the Royal Society of London B*, 213, 183–199.
- Tolhurst, D. J., Tadmor, Y. & Tang Chao (1992). The amplitude spectra of natural images. *Ophthalmic and Physiological Optics*, 12, 229–232.
- Watanabe, A., Mori, T., Nagata, S. & Hiwatashi, K. (1968). Spatial sine-wave responses of the visual system. *Vision Research*, 8, 1245–1263.
- Watson, A. B. (1992). Transfer of contrast sensitivity in linear visual networks. *Visual Neuroscience*, 8, 65–76.

Acknowledgement—Supported by NIH grant R29MH50588 to David J. Field